樹、早川 堯夫、森山 博由「贅肉は贅沢！?ヒト脂肪組織由来多系統前駆細胞の魅力」 【講演】Nov 23, 2014, 第５回生命機能研究会, 甲南大学ポートアイランドキャンパス, 神戸.

31) 宇田 純輝、森山 麻里子、早川 堯夫、森山 博由. オートファジー制御関連分子 BNIP3 は表皮分化ならびに表皮形態維持に重要な働きをする. [口頭発表] Nov 23, 2014, 第５回生命機能研究会, 甲南大学ポートアイランドキャンパス, 神戸. **[最優秀口頭発表賞受賞]**

32) 大森重成, 森山麻里子, 谷口祐紀, 深瀬尭哉, 松山晃文, 早川堯夫, 森山博由. ヒト脂肪組織由来多系統前駆細胞（hADMPC）を用いたドパミン産生細胞への誘導法の確立. [ポスター発表] Nov 23, 2014, 第５回生命機能研究会, 甲南大学ポートアイランドキャンパス, 神戸.

33) 石濱里穂, 森山麻里子, 鈴木格, 早川堯夫, 森山博由. ヒト脂肪組織由来多系統前駆細胞(hADMPC)を用いたメラノサイトの作製. [ポスター発表] Nov 23, 2014, 第５回生命機能研究会, 甲南大学ポートアイランドキャンパス, 神戸.

34) 百合祐樹,森山麻里子,早川堯夫,森山博由. 新規ヒト脂肪組織由来多能性前駆細胞に存在する OCT4 陽性細胞は真の多能性幹細胞たりうるのか？ [ポスター発表] Nov 23, 2014, 第５回生命機能研究会, 甲南大学ポートアイランドキャンパス, 神戸.

35) Junki Uda, Mariko Moriyama, Hiroyuki Moriyama, Takao Hayakawa. BNIP3 PLAYS CRUCIAL ROLES IN THE DIFFERENTIATION AND MAINTENANCE OF EPIDERMAL KERATINOCYTES. [Oral presentation] The 36th annual meeting of the molecular biology society of Japan. Nov 25-27, Pacifico-Yokohama, Yokohama, Japan.

36) Junki Uda, Mariko Moriyama, Hiroyuki Moriyama, Takao Hayakawa. BNIP3 PLAYS CRUCIAL ROLES IN THE DIFFERENTIATION AND MAINTENANCE OF EPIDERMAL KERATINOCYTES. [Poster presentation] The 36th annual meeting of the molecular biology society of Japan. Nov 25-27, Pacifico-Yokohama, Yokohama, Japan.

37) Shin Ishihara, Mariko Moriyama, Koichi Sakaguchi, Hanayuki Okura, Akifumi Matsuyama, Takao Hayakawa, Hiroyuki Moriyama. Role of Notch signaling in glycolysis regulation under hypoxic conditions. [Oral presentation] The 36th annual meeting of the molecular biology society of Japan. Nov 25-27, Pacifico-Yokohama, Yokohama, Japan.

38) Shin Ishihara, Mariko Moriyama, Koichi Sakaguchi, Hanayuki Okura, Akifumi Matsuyama, Takao Hayakawa, Hiroyuki Moriyama. Role of Notch signaling in glycolysis regulation under hypoxic conditions. [Poster presentation] The 36th annual meeting of the molecular biology society of Japan. Nov 25-27, Pacifico-Yokohama, Yokohama, Japan.

39) Riho Ishihama, Tadashi Michiyama, Hiroyuki Moriyama, Mariko Moriyama, Takao Hayakawa, Kiyofumi Ninomiya, Osamu Muraoka, Saowanee Chaipech[1,2] and Toshio Morikawa. Inhibitory Effects of Oligostilbenoids from Bark of *Shorea roxburghii* on Malignant Melanoma Cell Growth: Implications for a Candidate of Novel Topical Anticancer Agents. [Poster presentation] The 36th annual meeting of the molecular biology society of Japan. Nov 25-27, Pacifico-Yokohama, Yokohama, Japan.

40) Chiaki Sone, Mariko Moriyama, Hanayuki Okura, Akifumi Matsuyama, Takao Hayakawa, Hiroyuki Moriyama. Transdifferentiation of human adipose tissue-derived multilineage progenitor cells into insulin-producing cells. [Poster presentation] The 36th annual meeting of the molecular biology society of Japan. Nov 25-27, Pacifico-Yokohama, Yokohama, Japan.

41) Junki Uda, Mariko Moriyama, Hiroyuki Moriyama, Takao Hayakawa. BNIP3 PLAYS CRUCIAL ROLES IN THE DIFFERENTIATION AND MAINTENANCE OF EPIDERMAL KERATINOCYTES. [Oral presentation] The 39th annual meeting of the Japanese society for Investigative Dermatology. Dec 12-14, Expopark-Hankyu Osaka, Japan.

42) Mariko Moriyama. BNIP3 Plays Crucial Roles in the Differentiation and Maintenance of Epidermal Keratinocytes. Looking to the future of Notch signaling. December 18th, 2014. Institute for Protein Research, Osaka University, Osaka, Japan.

43) Kiyofumi Ninomiya, Toshio Morikawa, Taku Matsumoto, Mayumi Sueyoshi, Seiya Miyazawa, Shunsuke Saeki, Saowanee Chaipech, Takao Hayakawa, Osamu Muraoka. Anti-inflammatory effects and mode of action of prenylcoumarins from Thai natural medicine *Mammea siamensis*. The 27th International Conference on Polyphenols (ICP2014), (Nagoya, Japan), 2014.9.

44) Toshio Morikawa, Ikuko Hachiman, Kiyofumi Ninomiya, Hisashi Matsuda, Yuki Hata, Kaoru Sugawara, Yuri Sakata, Masayuki Yoshikawa, Takao Hayakawa, Osamu Muraoka. Antiallergic principles from *Myristica fragnans*: inhibitors of degranulation and TNF-α release in RBL-2H3 cells. The 27th International Conference on Polyphenols (ICP2014), (Nagoya, Japan), 2014.9.

45) Tadashi Michiyama, Horoyuki Moriyama, Mario Moriyama, Takao Hayakawa, Kiyofumi Ninomiya, Osamu Muraoka, Saowanee Chaipech, Toshio Morikawa. Inhibitory effects of oligostilbenoids

from bark of *Shorea roxburghii* on malignant melanoma cell growth: implications for a candidate of novel topical anticancer agents. The 27th International Conference on Polyphenols (ICP2014), (Nagoya, Japan), 2014.9.

46) Kiyofumi Ninomiya, Toru Minamino, Kaiten Ozeki, Natsuko Matsuo, Chihiro Kawabata, Takao Hayakawa, Toshio Morikawa. Effects of constituents from hooks of *Uncaria rhynchophylla* on neurite outgrowth and TNF-α-induced cell damage. The 8th JSP-CCTCM-KSP Joint Symposium on Pharmacognosy, (Fukuoka, Japan), 2014.9.

47) 第四回ウィリアムハンコック賞（4th William Hancock Award）受賞 基調講演, On January 27-29, 2015 WCBP2015 (the CASSS Board). Mayflower Renaissance Hotel, Washington, DC.

48) 2015 IABS meeting [International Regulatory Endeavor towards Sound Development of Human Cell Therapy Products], Challenges for developing a minimum consensus package plus case by case approaches for evaluating cell therapy products. February 18-19th, 2015. Hitotsubashi Hall, Tokyo, Japan.

49) 2015 IABS meeting [International Regulatory Endeavor towards Sound Development of Human Cell Therapy Products], Specifications. February 18-19th, 2015. Hitotsubashi Hall, Tokyo, Japan.

I. 知的財産権の出願・登録状況

1) 記載事項なし

II. 政策への提言

1) 「再生医療等の安全性の確保等に関する法律」、「再生医療等の安全性の確保等に関する法律施行令」及び「再生医療等の安全性の確保等に関する法律施行規則」の取扱いについて（平成26年10月31日医政研発1031第1号厚生労働省医政局研究開発振興課長通知）

2) 生物由来原料基準の一部を改正する件」（平成26年厚生労働省告示第375号）；

3) ヒト幹細胞を用いる臨床研究に関する指針（平成25年厚生労働省告示第317号）

4) ヒト（自己）体性幹細胞加工医薬品等の品質及び安全性の確保について（平成24年9月7日薬食発0907第2号）

5) ヒト（同種）体性幹細胞加工医薬品等の品質及び安全性の確保について（平成24年9月7日薬食発0907第3号）

6) ヒト（自己）iPS（様）細胞加工医薬品等の品質及び安全性の確保について（平成24年9月7日薬食発0907第4号）

7) ヒト（同種）iPS（様）細胞加工医薬品等の品質及び安全性の確保について（平成24年9月7日薬食発0907第5号）

8) ヒトES細胞加工医薬品等の品質及び安全性の確保について（平成24年9月7日薬食発0907第6号）（URL) http://www.nihs.go.jp/cgtp/cgtp/sec2/sispsc/html/regulation.html

9) 厚生科学審議会ヒト幹細胞を用いる臨床研究に関する検討の見直しに関する専門委員会での提言

10) 厚生労働省医薬食品局「薬事法改正における再生医療製品の位置づけに関する意見交換会」での提言

産業化支援に関する研究

研究分担者　辻　紘一郎　株式会社ツーセル　代表取締役社長

研究要旨
「関節軟骨病変に対する自己滑膜間葉系幹細胞由来三次元人工組織移植法」を、実用化の道筋にある厚生労働省の定める先進医療へスムーズな移行をさせるために、「滑膜幹細胞を原材料とする軟骨移植材（gMSC)」の薬事戦略相談を継続し、先進医療の申請準備をした。

A.研究目的

滑膜由来間葉系幹細胞（MSC）を用いた再生医療のレギュラトリーサイエンスについて、国内外の情報を収集、解析し、「関節軟骨病変に対する自己滑膜間葉系幹細胞由来三次元人工組織移植法」の先進医療への道筋を描き、実用化を目指す。

B.研究方法

2014年度は5月、10月、1月に「滑膜幹細胞を原材料とする軟骨移植材（gMSC)」の薬事戦略相談を実施。また、国際学会「World Stem Cell　Summit 2014」(米国・サンアントニオ,12 月)で再生医療の非臨床・臨床研究について情報収集を行った。

C.研究結果

大阪大学未来医療センターCPCにおいて、臨床試験に供する検体の製造場所として、模擬的な治験薬GMP査察を1月に実施し、PMDAによる指導・助言を受け、情報収集を行った。その結果、移植体の製造においては、高いレベルのベリフィケーションが必要となることを確認した。ベリフィケーションとは、検査や、特定の要求事項が満たされるということを客観的証拠で確認をすることである。欧州・北米ではこれに対応したシステム構築が進んでいる。国内は、品質は良質であるにもかかわらず、ベリフィケーションの不足により製造に供する材料として選択できない事例があり、諸外国に比べて立ち遅れていると考える。

D.考察

細胞は培地や材料の影響を受けてその性質が変わることから、製造材料が重要視されると考える。材料において、一貫性のある優れた品質のものを選択し、品質に関する明確な文書を収集し、さらにそのことを文書化することが、治療の品質を保証するという観点で重要であると考える。品質基準に個体差がある血清成分はこの対応が難しいと考える。

E.結論

先進医療として「関節軟骨病変に対する自己滑膜間葉系幹細胞由来三次元人工組織移植法」を実施し、普及をめざすにあたっては、治療データの分析等を行うことと並行して、ウシ血清を用いた製造方法を、一貫性のある品質であり、そのことが明確な文書で証明できる無血清培地を用いた製造方法に切り替えることが課題となる。また、培地や洗浄液、細胞剥離剤、細胞保存液等を精査し、ベリフィケーションの観点から選択することも課題となる。

従って、本研究で実施した「関節軟骨病変に対する自己滑膜間葉系幹細胞由来三次元人工組織移植法」の臨床研究をブラッシュアップさせて承認を得ることが、先進医療での実施の近道であり、最適な筋道であると考える。

F.研究発表

1．論文発表

なし

2．研究発表

1) 2014/3/4;無血清培地STK1及びSTK2を用いて増殖したイヌ滑膜由来間葉系幹細胞の特徴と他家移植による軟骨修復;第 13 回再生医療学会総会;前田悟,森川實,長谷川森一,邵金昌,大森亜樹,北山唯,高尾昌人,三木慎也,印南健,松下隆,辻紘一郎

2) 2014/3/5;軟骨組織再生治療材gMSC (guaranteed MSC) の保存条件の検討;第 13 回再生医療学会総会;岩本佳央梨,邵金昌,長谷川森一,鈴木美紀,松本昌也,前田悟,桂由紀,北山唯,谷川俊輔,加藤幸夫,辻紘一郎

G.知的財産権の出願・登録状況

なし

厚生労働科学研究費補助金（再生医療実用化研究事業）
（分担）研究報告書

外科的移植手技の開発・改良に関する研究

研究分担者　堀部　秀二　大阪府立大学　総合リハビリテーション　教授

研究要旨

自己滑膜間葉系幹細胞を用いた軟骨再生治療の低侵襲の移植手技の確立のための調査、研究を行った

研究分担者氏名・所属研究機関名及び所属研究機関における職名

（分担研究報告書の場合は、省略）

A．研究目的
自己滑膜間葉系幹細胞由来人工組織（ＴＥＣ）を用いた軟骨再生治療の低侵襲手術手技確立のための調査・研究を行なうことである。

B．研究方法
ＴＥＣを用いた軟骨再生治療の低侵襲手術手技確立のため、新しい外科手術の創出と共に、国内外の現状把握並びに情報交換を行った。

（倫理面への配慮）
ヘルシンキ宣言に基づく倫理的原則に留意、「ヒト幹細胞を用いる臨床研究に関する指針」を遵守

C．研究結果
ＴＥＣを用いた軟骨再生治療の低侵襲手術手技方法を完成し、今後それを実践していく。

D．考察
ＴＥＣを用いた軟骨再生治療の臨床応用の場で、出てくる可能性のある問題に十分留意し、情報収集する必要がある。

E．結論
今後、ＴＥＣを用いた軟骨再生治療の臨床応用を、実践していく。

F．健康危険情報
なし

G．研究発表
1．論文発表
AP-SMART 1:42-46, January 2014
Bone Joint Res. 3:241-5, 2014
J Orthop Sci. 19:925-32, 2014
J Orthop Traumatol.Jun 4, 2014
KSSTA, Jul 1, 2014
2．学会発表
APKASS meeting (2014.4, Nara)
ESSKA Congress (2014.5, Amsterdam)
JOA 2014 (2014.5, 神戸)
JOSKAS2014 (2014.7, 広島)
ASPI Congress (2014.8, Tokyo)

H．知的財産権の出願・登録状況
（予定を含む。）
なし

Ⅲ．研究成果の刊行に関する一覧表

研究成果の刊行に関する一覧表

書籍
該当なし

雑誌

発表者氏名	論文タイトル名	発表誌名	巻号	ページ	出版年
Shimomura K, Moriguchi Y, Murawski CD, Yoshikawa H, Nakamura N.	Osteochondral tissue engineering with biphasic scaffold: Current strategies and techniques.	Tissue Eng Part B	20	2291-304	2014
Ando W, Kutcher JJ, Kurawetz R, Sen A, Nakamura N, Frank CB, Hart DA	Clonal analysis of synovial fluid stem cells to characterize and identify stable mesenchymal stromal cell/mesenchymal progenitor cell phenotypes in a porcine model: a cell source with enhanced commitment to the chondrogenic lineage.	Cytotherapy	16	776-88	2014
Amano H, Iwahashi T, Suzuki T, Mae T, Nakamura N, Sugamoto K, Shino K, Yoshikawa H, Nakata K	Analysis of displacement and deformation of the medial meniscus with a horizontal tear using a three-dimensional computer model.	Knee Surg Sports Traumatol Arthrosc.	23	1153-60	2014
Sakai T, Koyanagi M, Nakae N, Kimura Y, Sanada Y, Nakamura N, Nakata K.	Evaluation of a new quadriceps strengthening exercise for the prevention of secondary cartilage injury in patients with pcl insufficiency: comparison of tibial movement in prone and sitting positions during the exercise.	Br J Sports Med.	48	656	2014

Shimomura K., Moriguchi, Y., Ando, W, Nansai, R., Fujie, H., Hart, D.A., Gobbi, A., Kita, K., Horibe, S, Shino, K., Yoshikawa, H., Nakamura, N.	Osteochondral Repair Using a Scaffold-Free Tissue-Engineered Construct Derived from Synovial Mesenchymal Stem Cells and a Hydroxyapatite-Based Artificial Bone.	Tissue Eng Part A.	21	2291-304	2014
Nakamura N., Hui J., Koizumi K., Yasui Y., Nishii T., Lad D., Karnatzikos G, Gobbi A.	Stem Cell Therapy in Cartilage Repair- Culture-free and Cell Culture-based Methods –	Oper Tech Orthop.	24	54-60	2014
Kita K, Tanaka Y, Toritsuka Y, Yonetani Y, Kanamoto T, Amano H, Nakamura N, Horibe S.	Patellofemoral chondral status after medial patellofemoral ligament reconstruction using second-look arthroscopy in patients with recurrent patellar dislocation.	J Orthop Sci.	19	925-32	2014
Shimomura K, Kanamoto T, Kita K, Akamine Y, Nakamura N, Mae T, Yoshikawa H, Nakata K.	Cyclic compressive loading on 3D tissue of human synovial fibroblasts upregulates prostaglandin E2 via COX-2 production without IL-1ß and TNF-α	Bone Joint Res.	3	280-8	2014
Gobbi A, Chaurasia S, Kamatzikos G, Nakamura N.	Matrix-induced Autologous Chondrocyte Implantation versus Multipotent Stem Cells for the Treatment of Large Patellofemoral Chondral Lesions: A Non-randomized Prospective Trial.	Cartilage	6	*82-97*	2014
中村亮介, 望月翔太, 中村憲正, 藤江裕道.	間葉系幹細胞由来組織再生材料と人工骨補填材による軟骨修復	臨床バイオメカニクスe	35	381-385	2014
池谷基志, 大家渓, 鈴木大輔, 小倉孝之, 小山洋一, 杉田憲彦, 中村憲正, 藤江裕道	組織再生材料（TEC）/コラーゲン複合体の引張特性	臨床バイオメカニクス	35	401-405	2014

谷　優樹, 大家　渓, 杉田憲彦, 中村憲正, 藤江裕道	ナノ周期構造上で作製した幹細胞自己生成組織（scSAT）の引張特性	臨床バイオメカニクス	35	407-411	2014
Kaneshiro, S., Ebina, K., Shi, K., Higuchi, C., Hirao, M., Okamoto, M., Koizumi, K., Morimoto, T., Yoshikawa, H., Hashimoto, J	IL-6 negatively regulates osteoblast differentiation through the SHP2/MEK2 and SHP2/Akt2 pathways in vitro.	J Bone Miner Metab.	32	378-392	2014
Minegishi, Y., Sakai, Y., Yahara, Y., Akiyama, H., Yoshikawa, H., Hosokawa, K., Tsumaki, N.	Cyp26b1 within the growth plate regulates bone growth in juvenile mice.	Biochem Biophys Res Commun	454	12-18	2014
Okamoto, M., Tanaka, H., Okada, K., Kuroda, Y., Nishimoto, S., Murase, T., Yoshikawa, H	Methylcobalamin promotes proliferation and migration and inhibits apoptosis of C2C12 cells via the Erk1/2 signaling pathway.	Biochem Biophys Res Commun	433	871-875	2014
Hirose, T. et al.	Presence of Neutrophil extracellular traps and Citrullinated histone H3 in the Blo-odstream of critically ill patients.	PLoS One	9(11)	e111755	2014
Hirose, T. et al.	Effecti-Veness of a simplifiedcardiopulmonary resuscitation training program for the non-medical staff of a university hospital	Scandinavian Journal of Trauma, Resuscitation and Emergency Medicine	22	31.	2014
Yamamoto, K. and Murakami, H.	Model based on skew normal distribution for square contingency tables with ordinal categories	Computational Statistics and Data Analysis	78	135-140	2014
Higuchi T, Miyagawa S, Pearson JT, Fukushima S, Saito A, Tsuchimochi H, Sonobe T, Fujii Y, Yagi N, Astolfo A, Shirai M, Sawa Y Sawa Y	Functional and Electrical Integration of Induced Pluripotent Stem Cell-Derived Cardiomyocytes in a Myocardial Infarction Rat Heart.	Cell Transplant.			2015

Kainuma S, Miyagawa S, Fukushima S, Pearson J, Chen YC, Saito A, Harada A, Shiozaki M, Iseoka H, Watabe T, Watabe H, Horitsugi G, Ishibashi M, Ikeda H, Tsuchimochi H, Sonobe T, Fujii Y, Naito H, Umetani K, Shimizu T, Okano T, Kobayashi E, Daimon T, Ueno T, Kuratani T, Toda K, Takakura N, Hatazawa J, Shirai M, Sawa Y.	BNIP3 Plays Crucial Roles in the Differentiation and Maintenance of Epidermal Keratinocytes	Mol Ther.	23(2)	374-86	2014
Kamata S, Miyagawa S, Fukushima S, Imanishi Y, Saito A, Maeda N, Shimomura I, Sawa Y.	Targeted Delivery of Adipocytokines Into the Heart by Induced Adipocyte Cell-Sheet Transplantation Yields Immune Tolerance and Functional Recovery in Autoimmune-Associated Myocarditis in Rats.	Circ J.	79(1)	169-79	2014
Kawamura T, Miyagawa S, Fukushima S, Yoshida A, Kashiyama N, Kawamura A, Ito E, Saito A, Maeda A, Eguchi H, Toda K, Lee JK, Miyagawa S, Sawa Y.	N-Glycans: Phenotypic Homology and Structural Differences between Myocardial Cells and Induced Pluripotent Stem Cell-Derived Cardiomyocytes.	PLoS One.	9(10)	e111064	2014
Uchinaka A, Kawaguchi N, Mori S, Hamada Y, Miyagawa S, Saito A, Sawa Y, Matsuura N. Tissue Inhibitor of Metalloproteinase-1 and -3 Improves Cardiac Function in an Ischemic Cardiomyopathy Model Rat	Tissue Inhibitor of Metalloproteinase-1 and -3 Improves Cardiac Function in an Ischemic Cardiomyopathy Model Rat.	Tissue Eng Part A.	20	3073-3084	2014

Takao Hayakawa, Takashi Aoi, Akihiro Umezawa, Keiya Ozawa, Yoji Sato, Yoshiki Sawa, Akifumi Matsuyama, Shinya Yamanaka, and Masayuki Yamato.	Study on Ensuring the Quality and Safety of Pharmaceuticals and Medical Devices Derived from the Processing of Autologous Human Somatic Stem Cells.	Regenerative Therapy		in press	2015
Takao Hayakawa, Takashi Aoi, Akihiro Umezawa, Keiya Ozawa, Yoji Sato, Yoshiki Sawa, Akifumi Matsuyama, Shinya Yamanaka, and Masayuki Yamato	Study on Ensuring the Quality and Safety of Pharmaceuticals and Medical Devices Derived from the Processing of Allogenic Human Somatic Stem Cells.	Regenerative Therapy		2015 in press	2015
Takao Hayakawa, Takashi Aoi, Akihiro Umezawa, Keiya Ozawa, Yoji Sato, Yoshiki Sawa, Akifumi Matsuyama, Shinya Yamanaka, and Masayuki Yamato.	Study on Ensuring the Quality and Safety of Pharmaceuticals and Medical Devices Derived from Processing of Autologous Human Induced Pluripotent Stem Cell (-Like Cells)	Regenerative Therapy		2015 in press	2015
Takao Hayakawa, Takashi Aoi, Akihiro Umezawa, Keiya Ozawa, Yoji Sato, Yoshiki Sawa, Akifumi Matsuyama, Shinya Yamanaka, and Masayuki Yamato.	Study on Ensuring the Quality and Safety of Pharmaceuticals and Medical Devices Derived from Processing of Allogenic Human Induced Pluripotent Stem Cell (-Like Cells).	Regenerative Therapy		2015 in press	2015

Takao Hayakawa, Takashi Aoi, Akihiro Umezawa, Keiya Ozawa, Yoji Sato, Yoshiki Sawa, Akifumi Matsuyama, Shinya Yamanaka, and Masayuki Yamato.	Study on Ensuring the Safety and Quality of Pharmaceuticals and Medical Devices Derived from the Processing of Human Embryonic Stem Cells.	Regenerative Therapy		2015 in press	2015
Moriyama H, Moriyama M, Isshi H, Ishihara S, Okura H, Ichinose A, Ozawa T,Matsuyama A, Hayakawa T.	Role of notch signaling in the maintenance of humanmesenchymal stem cells under hypoxic conditions.	Stem Cells Dev.	23(18)	2211-24	2014
Moriyama M, Moriyama H, Uda J, Matsuyama A, Osawa M, Hayakawa T.	BNIP3 plays crucial roles in the differentiation and maintenance of epidermal keratinocytes.	J Invest Dermatol.	134(6):	1627-35.	2014
Takayama K, Kawabata K, Nagamoto Y, Inamura M, Ohashi K, Okuno H, Yamaguchi T, Tashiro K, Sakurai F, Hayakawa T, Okano T, Furue MK, Mizuguchi H.	CCAAT/enhancer binding protein-mediated regulation of TGFß receptor 2 expression determines the hepatoblast fate decision.	Development	141(1):	91-100	2014
Yagi Y, Kakehi K, Hayakawa T, Suzuki S.	Application of microchip electrophoresis sodium dodecyl sulfate for the evaluation of change of degradation species of therapeutic antibodies in stability testing.	Anal Sci.	30(4)	483-8	2014

Toshio Morikawa, Kiyofumi Ninomiya, Katsuya Imura, Takahiro Yamaguchi, Yoshinori Akagi, Masayuki Yoshikawa, Takao Hayakawa, Osamu Muraoka,	Hepatoprotective triterpenes from traditional Tibetan medicine *Potentilla anserina*.	*Phytochemistry*	102	169—181	2014
Toshio Morikawa, Yusuke Nakanishi, Kiyofumi Ninomiya, Hisashi Matsuda, Souichi Nakashima, Hisako Miki, Yu Miyashita, Masayuki Yoshikawa, Takao Hayakawa, Osamu Muraoka	Dimeric pyrrolidinoindoline-type alkaloids with melanogenesis inhibitory activity in flower buds of *Chimonanthus praecox*.	*J. Nat. Med.*	68	539—549	2013
Takashi Kanamoto・Yoshinari Tanaka・Yasukazu Yonetani・Keisuke Kita・Hiroshi Amano・Masashi Kusano・Shinji Hirabayashi・Shuji Horibe	Anterior knee symptoms after double-bundle ACL reconstruction with hamstring tendon autografts: an ultrasonographic and power Doppler investigation	Knee Surg Sports Traumatol Arthrosc			2014
Takashi Kanamoto・Yoshinari Tanaka・Yasukazu Yonetani・Keisuke Kita・Hiroshi Amano・Masashi Kusano・Mie Fukamatsu・Shinji Hirabayashi・Shuji Horibe	Patellar mobility can be reproducibly measured using ultrasound	J Orthopaed Traumatol	16	55-8	2014

Keisuke Kita・Yoshinari Tanaka・Yukiyoshi Toritsuka・Yasukazu Yonetani・Takashi Kanamoto・Hiroshi Amano・Norimasa Nakamura・Shuji Horibe	Patellofemoral chondral status after medial patellofemoral ligament reconstruction using second-look arthroscopy in patients with recurrent patellar dislocation	J Orthop Sci	19(6)	925-932	2014
T. Kanamoto, Y. Shiozaki, Y. Tanaka, Y. Yonetani, S. Horibe	The use of MRI in pre-operative evaluation of anterior talofibular ligament in chronic ankle instability	Bone Joint Res.E	3(8)	241-5	2014

Ⅳ．研究成果の刊行物・別冊

TISSUE ENGINEERING: Part A
Volume 00, Number 00, 2014

DOI: 10.1089/ten.tea.2013.0414

Original Article

Osteochondral Repair Using a Scaffold-Free Tissue-Engineered Construct Derived from Synovial Mesenchymal Stem Cells and a Hydroxyapatite-Based Artificial Bone

Kazunori Shimomura, MD, PhD,[1] Yu Moriguchi, MD, PhD,[1] Wataru Ando, MD, PhD,[2] Ryosuke Nansai,[3] Hiromichi Fujie, PhD,[3,4] David A. Hart, PhD,[5] Alberto Gobbi, MD,[6] Keisuke Kita, MD, PhD,[1] Shuji Horibe, MD, PhD,[7] Konsei Shino, MD, PhD,[8] Hideki Yoshikawa, MD, PhD,[1] and Norimasa Nakamura, MD, PhD[1,9,10]

For an ideal osteochondral repair, it is important to facilitate zonal restoration of the subchondral bone and the cartilage, layer by layer. Specifically, restoration of the osteochondral junction and secure integration with adjacent cartilage could be considered key factors. The purpose of the present study was to investigate the feasibility of a combined material comprising a scaffold-free tissue-engineered construct (TEC) derived from synovial mesenchymal stem cells (MSCs) and a hydroxyapatite (HA) artificial bone using a rabbit osteochondral defect model. Osteochondral defects were created on the femoral groove of skeletally mature rabbits. The TEC and HA artificial bone were hybridized to develop a combined implant just before use, which was then implanted into defects ($N=23$). In the control group, HA alone was implanted ($N=18$). Histological evaluation and micro-indentation testing was performed for the evaluation of repair tissue. Normal knees were used as an additional control group for biomechanical testing ($N=5$). At hybridization, the TEC rapidly attached onto the surface of HA artificial bone block, which was implantable to osteochondral defects. Osteochondral defects treated with the combined implants exhibited more rapid subchondral bone repair coupled with the development of cartilaginous tissue with good tissue integration to the adjacent host cartilage when assessed at 6 months post implantation. Conversely, the control group exhibited delayed subchondral bone repair. In addition, the repair cartilaginous tissue in this group had poor integration to adjacent cartilage and contained clustered chondrocytes, suggesting an early osteoarthritis (OA)-like degenerative change at 6 months post implantation. Biomechanically, the osteochondral repair tissue treated with the combined implants at 6 months restored tissue stiffness, similar to normal osteochondral tissue. The combined implants significantly accelerated and improved osteochondral repair. Specifically, earlier restoration of subchondral bone, as well as good tissue integration of repair cartilage to adjacent host tissue could be clinically relevant in terms of the acceleration of postoperative rehabilitation and longer-term durability of repaired articular surface in patients with osteochondral lesions, including those with OA. In addition, the combined implant could be considered a promising MSC-based bio-implant with regard to safety and cost-effectiveness, considering that the TEC is a scaffold-free implant and HA artificial bone has been widely used in clinical practice.

[1]Department of Orthopaedics, Osaka University Graduate School of Medicine, Suita, Osaka, Japan.
[2]Department of Orthopaedics, Kansai Rosai Hospital, Amagasaki, Hyogo, Japan.
[3]Biomechanics Laboratory, Department of Mechanical Engineering, Kogakuin University, Hachioji, Tokyo, Japan.
[4]Division of Human Mechatronics Systems, Faculty of System Design, Tokyo Metropolitan University, Hino, Tokyo, Japan.
[5]McCaig Institute for Bone and Joint Health, University of Calgary, Calgary, Canada.
[6]Orthopaedic Arthroscopic Surgery International, Milan, Italy.
[7]Graduate School of Comprehensive Rehabilitation, Osaka Prefecture University, Habikino, Osaka, Japan.
[8]Department of Physical Therapy, Osaka Yukioka College of Health Science, Ibaraki, Osaka, Japan.
[9]Institute for Medical Science in Sports, Osaka Health Science University, Osaka, Japan.
[10]Center for Advanced Medical Engineering and Informatics, Osaka University, Suita, Osaka, Japan.

Introduction

OSTEOARTHRITIS (OA) is a common disease that causes joint pain, joint deformity, and functional disability, and it could potentially affect the quality of life of elderly populations worldwide.[1] There are several clinical options for the treatment of OA such as total joint replacement, osteotomy, and osteochondral transplantation, according to the severity of the joint destruction. Moreover, several biological approaches such as the use of biologics and tissue-engineered materials have been recently evaluated.[2–6]

For an ideal repair of osetochondral lesions with the involvement of subchondral bone pathology, it is important to regenerate subchondral bone, and to facilitate zonal restoration of cartilage and subchondral bone, layer by layer.[5,7,8] As a strategy to regenerate these structures layer by layer, biphasic or triphasic constructs have been developed.[9–17] These constructs have been reported to contribute to good osteochondral repair *in vivo*, while there are still several concerns associated with the complicated process of manufacturing implants such as cell seeding, cell differentiation and combining materials, and the long-term safety of these constructs due to the involvement of chemical- or animal-derived materials. Therefore, a novel construct that overcomes such potential problems is preferable for clinical applications. The process of manufacturing implants should be simplified. The use of chemical- or animal-free materials could be considered an ideal method to meet such requirements.

Artificial bones generated from hydroxyapatite (HA) or beta-tricalcium phosphate (β-TCP) have been widely used for clinical treatment of bone defects after fractures or after resection of bone tumors.[18–20] We have developed a novel fully interconnected HA artificial bone with a sufficient initial strength, as well as an excellent bone-formation capacity,[19,21] and previously reported the feasibility of this implant to repair subchondral bone.[18] In addition, we have developed a scaffold-free three-dimensional tissue-engineered construct (TEC) composed of allogenic mesenchymal stem cells (MSCs) derived from the synovium and extracellular matrices (ECMs) synthesized by the cells,[22] and demonstrated the feasibility of the resultant TEC to facilitate cartilage repair in a large animal model.[23,24] These TEC are developed without an artificial scaffold, and, thus, their implantation could eliminate or minimize the risk of potential side effects induced by extrinsic chemical or biological materials. Furthermore, such TEC are highly adherent to cartilage matrix, and secure integration of the TEC to adjacent cartilage tissue is observed after implantation.[23–25] Therefore, combined constructs of TEC and the fully interconnected HA-based artificial bone may effectively repair an osteochondal lesion with zonal restoration. The purpose of the present study was to test this hypothesis using a rabbit osteochondral defect model.

Materials and Methods

All procedures of this study followed the Declaration of Helsinki principles.

Harvest of synovial tissue and isolation of the cells

All animal experiments were approved by the Animal Laboratory of our institute. Rabbit synovial membranes were obtained aseptically from the knee joints of skeletal mature (24 weeks of age) female rabbits within 12 h of death. The cell isolation protocol was essentially that which was previously used for the isolation of human synovial-derived MSC.[22] Briefly, synovial membrane specimens were rinsed with sterile phosphate-buffered saline (PBS), minced meticulously, and digested with 0.4% collagenase XI (Sigma-Aldrich, St. Louis, MO) for 2 h at 37°C. After neutralization of the collagenase with growth medium containing high-glucose Dulbecco's modified Eagle's medium (HG-DMEM; Wako, Osaka, Japan) that was supplemented with 10% fetal bovine serum (FBS; HyClone, Logan, UT) and 1% penicillin/streptomycin (Gibco BRL, Life Technologies, Inc., Carlsbad, CA), the cells were collected by centrifugation, washed with PBS, re-suspended in growth medium, and plated in culture dishes with growth media mentioned earlier. The characteristics of the rabbit cells were similar to those of the human synovium-derived MSC with regard to morphology, growth characteristics, and multipotent differentiation capacity (to osteogenic, chondrogenic, and adipogenic lineages).[22,26] For expansion, cells were cultured in the growth medium at 37°C in a humidified atmosphere of 5% CO_2. The medium was replaced once per week. After 7–10 days of primary culture, when the cells reached confluence, they were washed twice with PBS, harvested by treatment with trypsin-EDTA (0.25% trypsin and 1 mM EDTA; Gibco BRL, Life Technologies, Inc.), and replated at 1:3 dilutions for the first subculture. Cell passages were continued in the same manner with 1:3 dilutions when cultures reached near confluence. Cells at passages 3–7 were used in the present studies.

Development of the TECs

Synovial MSCs were plated on six-well plates (9.6 cm^2) at a density of 4.0×10^5 cells/cm^2 in growth medium containing 0.2 mM ascorbate-2-phosphate (Asc-2P), an optimal concentration from earlier studies.[22–24] Within a day, the cells became confluent. After an additional 7–14 days in culture, a complex of the cultured cells and the ECM synthesized by the cells was detached from the culture dish by the application of shear stress using gentle pipetting. The detached monolayer complex was left in suspension to form a three-dimensional structure by active tissue contraction, and kept in cultured medium until implantation. This tissue was termed a basic scaffold-free three-dimensional TEC. Such TECs were sufficiently strong to be sustained against surgical handling as shown in our previous study.[22]

Development of the combined implant made of the TEC and artificial bone

A fully interconnected porous synthetic HA [5 mm in diameter, 4 mm in height (NEOBONE®; MMT Co. Ltd., Osaka, Japan)] was prepared as an artificial bone. The HA ceramics have 75% porosity and an interconnected porous structure, with more than 90% of the pores being connected by channels that are large enough for cells or tissue to penetrate. The surfaces of the pores are very smooth and the HA particles are tightly bound together, which provides a rather high mechanical compressive strength of about 10 MPa despite the porosity of this substance. This material displays good osteoconduction and bone ingrowth in animals and is also in clinical use.[18,19,21]

We prepared individual TEC to be hybridized with an artificial bone. TEC were detached from culture dishes just before the animal surgery, and combined with the artificial bone without any adhesive, to create a biphasic construct (Fig. 1a). The TEC immediately bonded to the surface of the artificial bone block and developed a stable complex that was maintained throughout the experiment.

Implantation of the combined implants to osteochondral defects

Forty one skeletal mature New Zealand White rabbits were kept in individual cages and had free access to food pellets and water. The rabbits were anesthetized by an intravenous injection of 1 mL of pentobarbital [50 mg/mL (Nembutal®; Dainippon Pharmaceutical Co. Ltd., Osaka, Japan)] and an intramuscular injection of 1 mL of xylazine hydrochloride [25 mg/mL (Seractal®; Bayer, Germany)]. After shaving, disinfection, and draping, a straight 3 cm-long medial parapatellar incision was made over the right knee; the patella was gently dislocated laterally; and the femoral groove was exposed. Full-thickness articular osteochondral defects, 5 mm in diameter and 6 mm in depth, were created mechanically in the femoral groove of the right distal femur using a drill at moderate speed, while irrigating the site with a room temperature saline solution, so as to prevent thermal damage to the surrounding bone and cartilage (Fig. 1b). The TEC and artificial bone was combined just before implantation as described earlier, and then, the combined constructs were implanted into the defects in 23 right knees by a press-fit technique (TEC group). In the control defect group, the defects were implanted with the artificial HA bone alone for 18 right knees (Fig. 1c). All animals were immobilized for 7 days, and euthanized under anesthesia at 1, 2, and 6 months after surgery. The distal femur of the animals, including the grafted site (18 specimens from the TEC group and 13 specimens from the control group), was used for histological analysis. The other specimens (five specimens from the TEC group and five specimens from the control group) were subjected to biomechanical testing. Five left knees were used as untreated normal controls for the biomechanical testing.

Histological evaluation of repaired tissue

For histological evaluation, tissue was fixed with 10% neutral buffered formalin, decalcified with K-CX (Falma, Tokyo, Japan), and embedded in paraffin, and 3 μm sections were prepared. The sections were stained with hematoxylin and eosin (H&E) and Toluidine Blue staining.

The histology of repaired tissue at 1, 2, and 6 months was evaluated by the modified O'Driscoll score for cartilage and subchondral bone repair.[27–29] The category "Toluidine Blue staining" was substituted for "Safranin O staining." Moreover, new criteria categories "cellular morphology" and "exposure of subchondral bone" were implemented in addition to the categories associated with subchondral bone repair. With regard to the "cellular morphology" category, normal subchondral bone repair was given a score of 2, a repair tissue mixed with cartilage-like tissue was a score of 1, and a repair tissue mixed with fibrous tissue was a score of 0. With regard to the "exposure of subchondral bone" category, no subchondral bone exposure was a score of 2, subchondral bone exposure at one side of the borders between repair tissue and adjacent cartilage was a score of 1, and subchondral bone exposure at both sides was a score of 0. The repair tissue was divided into three parts of 2 mm width, which consisted of the center area and both border areas, and then each area was evaluated by the modified O'Driscoll score. Based on these scores, each category was evaluated for "overall evaluation," which averaged the center area and both border areas. Moreover, the score of the central area as "central area" was also evaluated, and the average score of both border areas as "border area." The categories "bonding to adjacent cartilage," "freedom from degeneration of adjacent cartilage," and "exposure of subchondral bone," which do not involve spatial differences, were evaluated only as "overall evaluation."

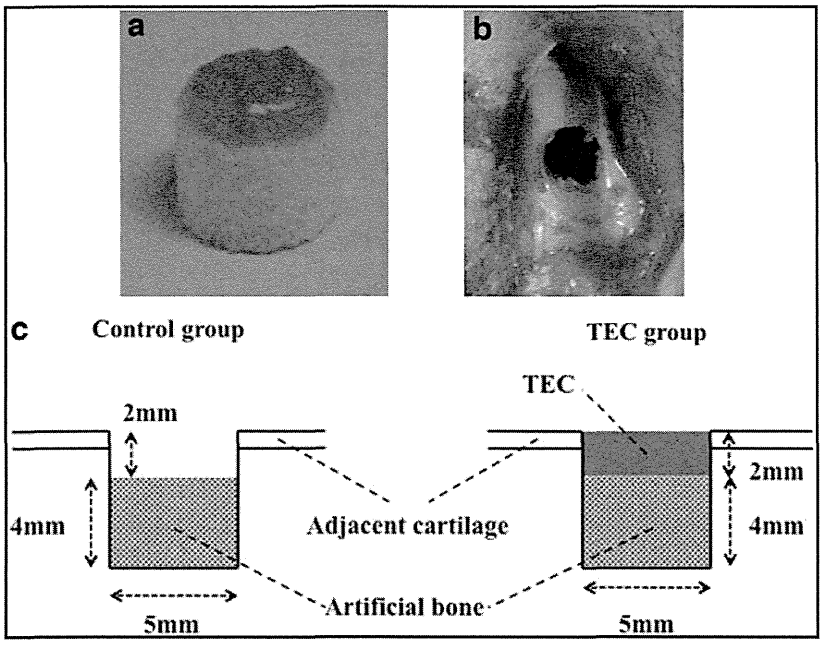

FIG. 1. **(a)** The combined implant generated with a tissue-engineered construct (TEC) and an artificial bone. **(b)** Osteochondral defects in the femoral groove of the rabbit knee. **(c)** Schematic representation of implanted materials in the control (hydroxyapatite, HA-bone alone) and the TEC-HA bone group. Color images available online at www.liebertpub.com/tea

Biomechanical testing

Cylindrically shaped specimens that were 4 mm in diameter and 5 mm in depth were removed from the graft sites of defects from both the TEC group and the control group. Similarly, cylindrically shaped specimens were removed from the central femoral groove of untreated normal knees. Micro-indentation testing was performed on the specimens using an Atomic Force Microscope (AFM) (Nanoscope IIIa; Veeco Instruments, Santa Barbara, CA) and a silicon nitride probe (spring constant: 0.06 N/m, DNP-S; Veeco Instruments). Each specimen was mounted on the sample stage of the AFM and soaked in saline solution at room temperature. Micro-indentation testing was performed on the specimens at an indentation rate of 5.12 μm/s.

Statistical analysis

Statistical analysis was performed using analysis of variance followed by *post-hoc* testing for the postoperative changes of total histological scores and biomechanical testing (Figs. 6a, b and 7). The comparison of results for other parameters between the control and TEC groups was analyzed by the Mann–Whitney *U* test (Tables 1 and 2). The results are presented as mean ± SD. The data were analyzed with JMP 9 (SAS Institute, Cary, NC), and significance was set at $p < 0.05$.

TABLE 1. HISTOLOGICAL EVALUATION FOR CARTILAGE REPAIR

Histological score description	*1 month postop*			*2 months postop*			*6 months postop*		
	Control (N=4)	*TEC (N=6)*	p *value*	*Control (N=4)*	*TEC (N=7)*	p *value*	*Control (N=5)*	*TEC (N=5)*	p *value*
Cellular morphology									
Overall evaluation	0	1.22±0.50	**0.0073**	1.67±0.39	3.14±0.63	**0.0109**	1.47±1.28	3.20±0.30	**0.0343**
Central area	0	0.33±0.82	0.4142	1.00±1.15	2.86±1.57	0.0716	1.60±2.19	3.60±0.089	0.1202
Border area	0	1.67±0.52	**0.0062**	2	3.29±0.76	**0.0152**	1.40±1.14	3.00±0.71	**0.0393**
Toluidine Blue staining									
Overall evaluation	0	0.92±0.37	**0.0073**	1.09±0.42	2.14±0.51	**0.0171**	1.27±0.86	2.67±0.47	**0.0196**
Central area	0	0.33±0.52	0.2207	0.50±0.58	2.29±1.11	**0.0309**	1.20±1.64±	3	**0.0495**
Border area	0	0.92±0.38	**0.0073**	1.38±0.48	2.07±0.61	0.0716	1.30±0.84	2.10±0.42	0.0827
Surface regularity									
Overall evaluation	0.42±0.50	1.89±0.66	**0.0131**	1.83±0.43	2.24±0.42	0.1420	1.20±0.65	1.80±1.30	0.0731
Central area	0.25±0.50	2.17±0.75	**0.0114**	2.75±0.50	2.71±0.49	0.9029	2.40±0.89	2.80±0.45	0.4386
Border area	0.50±0.58	1.75±0.69	**0.0159**	1.38±0.48	2.00±0.58	0.0977	0.60±0.65	1.70±0.91	0.0723
Structural integrity									
Overall evaluation	0.42±0.50	1.50±0.36	**0.0131**	1.09±0.42	1.52±0.38	0.1001	0.73±0.43	1.53±0.38	**0.0174**
Central area	0.50±0.58	1.83±0.41	0.0109	2	2	1.0000	1.60±0.89	2	0.3173
Border area	0.38±0.48	1.33±0.41	0.0201	0.63±0.63	1.29±0.57	0.1001	0.30±0.27	1.30±0.57	**0.0170**
Thickness									
Overall evaluation	0.50±0.58	1.39±0.57	0.0765	1.83±0.34	1.52±0.38	0.1862	0.80±0.65	1.40±0.28	0.1071
Central area	0.50±0.58	1.50±0.55	**0.0372**	2	1.71±0.49	0.2598	1.20±1.10	1.80±0.45	0.3662
Border area	0.50±0.58	1.33±0.61	0.0765	1.75±0.50	1.43±0.45	0.2621	0.60±0.55	1.20±0.27	0.0652
Bonding to adjacent cartilage									
Overall evaluation	0.13±0.25	1.50±0.45	**0.0089**	0.38±0.48	1.64±0.48	**0.0109**	0.30±0.27	1.50±0.61	**0.0167**
Hypocellularity									
Overall evaluation	1.00±1.28	2.89±0.27	**0.0121**	3	3	1.0000	1.80±1.12	2.74±0.15	0.0837
Central area	0.25±0.50	2.67±0.82	**0.0078**	3	3	1.0000	1.80±1.30	3	0.0539
Border area	1.25±1.50	3	**0.0177**	3	3	1.0000	1.80±1.15	2.60±0.22	0.1797
Chondrocyte clustering									
Overall evaluation	0	0.17±0.41	0.4142	0.42±0.50	1.24±0.46	**0.0325**	0.40±0.37	1.53±0.30	**0.0074**
Central area	0	0.17±0.41	0.4142	0.25±0.50	1.29±0.76	**0.0453**	0.80±0.84	2	**0.0177**
Border area	0	0.17±0.41	0.4142	0.5±0.58	1.21±0.39	**0.0482**	0.20±0.27	1.30±0.45	**0.0072**
Freedom from degeneration of adjacent cartilage									
Overall evaluation	2.88±0.25	3	0.2207	2.38±0.25	2.71±0.27	0.0763	1.60±0.22	2.40±0.22	**0.0073**
Total score	5.34±2.59	14.22±2.02	**0.0103**	13.67±2.10	19.16±2.33	**0.0179**	9.56±5.17	19.03±2.15	**0.0119**

Bold values show statistically significant differences between control group and TEC group.

TABLE 2. HISTOLOGICAL EVALUATION FOR SUBCHONDRAL BONE REPAIR

	1 month postop			*2 months postop*			*6 months postop*		
Histological score description	*Control (N=4)*	*TEC (N=6)*	p *value*	*Control (N=4)*	*TEC (N=7)*	p *value*	*Control (N=5)*	*TEC (N=5)*	p *value*
Subchondral bone alignment									
Overall evaluation	0	0	1.0000	0.67±0.54	1.67±0.34	**0.0144**	0.73±0.87	1.27±0.43	0.3305
Central area	0	0	1.0000	0.25±0.50	1.57±0.79	**0.0249**	0.80±0.84	1.00±0.71	0.6501
Border area	0	0	1.0000	0.88±0.85	1.71±0.39	0.0904	0.70±0.97	1.40±0.55	0.2328
Bone integration									
Overall evaluation	0	0	1.0000	0.75±0.57	1.79±0.39	**0.0130**	1.47±0.84	1.87±0.18	0.4189
Central area	0	0	1.0000	0.25±0.50	1.43±0.98	0.0601	1.20±0.84	1.60±0.55	0.4189
Border area	0	0	1.0000	1.00±0.91	1.57±0.79	0.2150	1.60±0.89	2	0.3173
Bone infiltration into defect area									
Overall evaluation	0	0	1.0000	0.67±0.54	1.48±0.50	**0.0437**	1.60±0.55	1.80±0.18	0.7290
Central area	0	0	1.0000	0.25±0.50	1.29±0.95	0.0831	1.20±0.84	1.40±0.55	0.7290
Border area	0	0	1.0000	0.88±0.85	1.79±0.39	0.0629	1.80±0.45	2	0.3173
Tidemark continuity									
Overall evaluation	0	0	1.0000	0	0.67±0.67	0.0763	0.40±0.37	1.20±0.38	**0.0192**
Central area	0	0	1.0000	0	0.86±1.07	0.1432	0.60±0.89	1.20±0.84	0.2685
Border area	0	0	1.0000	0	0.57±0.53	0.0708	0.30±0.27	1.20±0.27	**0.0071**
Cellular morphology									
Overall evaluation	0	0	1.0000	0.84±0.33	1.76±0.32	**0.0104**	1.47±0.51	1.60±0.28	0.8266
Central area	0	0	1.0000	0.25±0.50	1.43±0.79	**0.0355**	1.00±1.00	1.40±0.55	0.5023
Border area	0	0	1.0000	1.13±0.63	1.93±0.19	**0.0281**	1.70±0.45	1.70±0.45	1.0000
Exposure of subchondral bone									
Overall evaluation	1.00±1.15	1.67±0.52	0.2708	2	1.71±0.49	0.2598	0.80±0.84	1.80±0.45	0.0539
Total score	1.00±1.15	1.67±0.52	0.2708	4.92±1.91	9.07±1.84	**0.0140**	6.47±3.20	9.54±1.26	0.0937

Bold values show statistically significant differences between control group and TEC group.

Results

Macroscopic evaluation of repair tissue

At 1 month after surgery, bare artificial bones were exposed at the surface of the implanted area in all subjects of the control group (Fig. 2a, arrow heads). Conversely, the defects were uniformly covered with repair tissue in the TEC group. The periphery of the repair tissue was white and in contrast, the center area was translucent (Fig. 2b). At 2 months after surgery, the defects were covered with a white colored repair tissue in both groups. However, more precise observation revealed that the repair tissue in the control group exhibited surface cracks or subchondral bone exposure between the repair tissue and the adjacent cartilage (Fig. 2c, arrow heads). In the TEC group, although the margin line was obvious, there were no overt cracks or subchondral bone exposure detected within the repair tissue (Fig. 2d). At 6 months post surgery, obvious cracks or

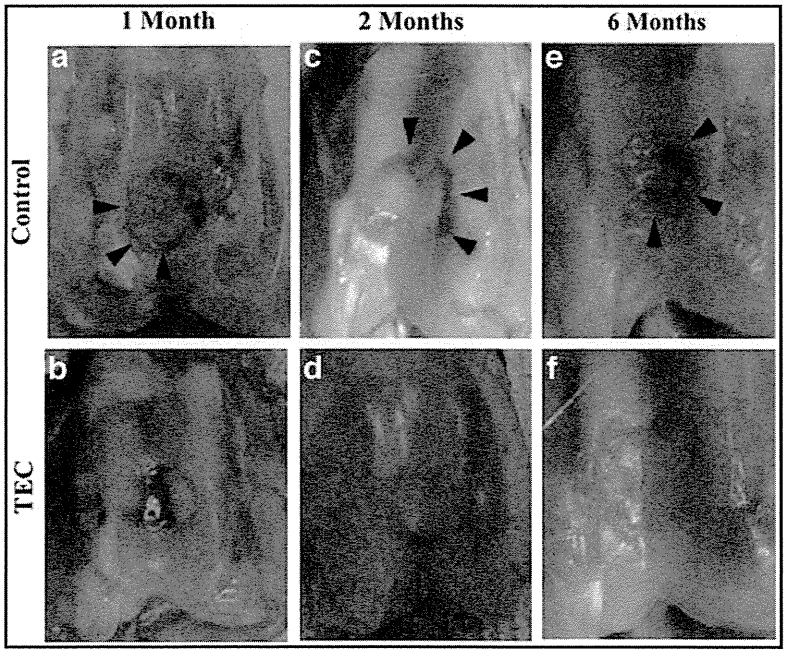

FIG. 2. Macroscopic view of repair tissues at 1, 2, and 6 months after surgery treated with artificial HA bone alone (**a, c, e,** respectively) or the TEC-HA combined implant (**b, d, f,** respectively). At 1 month after surgery, bare artificial bones were exposed at the surface of the implanted area in the control group (**a**). At 2 and 6 months, the control group showed obvious cracks or subchondral bone exposure between repair tissue and the adjacent cartilage (**c, e,** arrow heads). Conversely, such defects were covered with repair tissue in the TEC-HA group out to 6 months (**b, d, e**). Color images available online at www.liebertpub.com/tea

subchondral bone exposure between repair tissue and the adjacent cartilage were still observed in the control group samples (Fig. 2e, arrow heads). In contrast, the repair tissue in the TEC group consistently showed a continuous surface beyond the surface of adjacent cartilage. The margin line between the repair tissue and the adjacent cartilage was less distinguishable (Fig. 2f).

Histological evaluation of repair tissue

At 1 month after surgery, bare artificial bone was exposed partially at the surface of implanted area without repair tissue in the control group (Fig. 3a, arrows). Conversely, the defects were consistently repaired with thick fibrous tissues with good integration to the adjacent host tissue in the TEC group (Fig. 3b). In higher magnification views, new bone formation was observed at the bilateral peripheral margin of implanted TEC adjacent to the surrounding host bone marrow and the surface of the artificial bone (Fig. 3c, arrow heads). Notably, the development of immature chondrogenic tissue with round-shaped cells in lacuna were simultaneously observed within the implanted TEC surrounding the area of new bone formation (Fig. 3d), while fibrous tissue was observed in the center area of the TEC (Fig. 3e).

At 2 months, defects were filled with a fibrous-like tissue with moderate Toluidine blue staining, but bone formation was rarely observed on the surface of the artificial bone in the control group samples (Fig. 4a, b). In contrast, new bone formation within the TEC further extended from the bilateral peripheral border toward the central area on the surface of the artificial bone (Fig. 4c, arrows). It should be noted that the level of the upper surface of the newly synthesized bone was similar to that of the adjacent uninjured subchondral bone (Fig. 4c, d, dotted lines). In higher magnification views, there was poor integration of the repair tissue with the adjacent host cartilage in the control group samples (Fig. 4e). The repair tissue in the control group contained round-shaped cells in lacuna, but with weak Toluidine Blue-stained ECM, and, thus, the development of chondrogenic tissue appeared insufficient or less advanced (Fig. 4f, j). Conversely, the repair tissue in the TEC group samples exhibited hyaline cartilage-like repair (Fig. 4h, k) with good tissue integration to the adjacent host cartilage (Fig. 4g). Similar to 1 month post implantation, chondrogenic tissue with Toluidine Blue-positive ECM was observed to have developed in contact with newly synthesized bone (Fig. 4i).

At 6 months, osteochondral repair had progressed in the control group (Fig. 5a, b); however, the repair tissue still

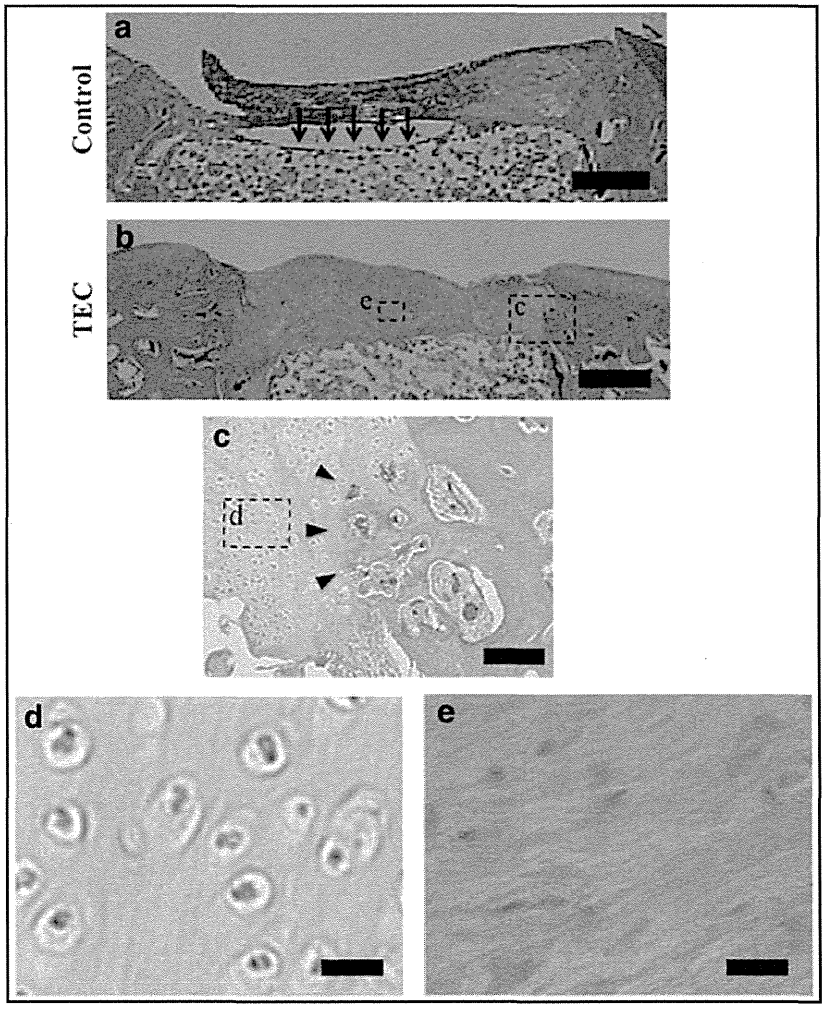

FIG. 3. Hematoxylin and eosin (H&E) staining of repair tissues implanted with artificial bone alone **(a)** or the combined implant **(b)**. The osteochondral defects treated with the combined implants were repaired with a thick fibrous-like tissue. Arrows show that bare artificial bone was exposed at the surface of implanted area without repair tissue in the control group **(a)**. Bar = 1 mm. Higher magnification views showed that ossification was partially observed inside the implanted TEC adjacent to host bone marrow on the surface of the artificial bone **(c**, arrowheads). Bar = 100 μm. Notably, the development of an immature chondrogenic tissue with round-shaped cells in lacuna was simultaneously observed within the implanted TEC surrounding the area of new bone formation **(d)**, while fibrous tissue was observed in the center of the TEC **(e)**. Bar = 20 μm. Color images available online at www.liebertpub.com/tea